Three-dimensional structure of the Earth from splitting in free-oscillation spectra

Domenico Giardini, Xiang-Dong Li & John H. Woodhouse

Department of Earth and Planetary Sciences, Harvard University, Cambridge, Massachusetts, 02138, USA

Observations of splitting in free oscillations spectra can be used to constrain the three-dimensional distribution of heterogeneity in the Earth. Modes sampling mainly the Earth's mantle are compatible with the distributions of mantle heterogeneity inferred from P-wave travel times. The anomalously large splitting of modes penetrating deeply into the core requires large departures from sphericity which are difficult to accommodate within the framework of an isotropic model; it is argued that anisotropy of the inner core offers the most natural explanation of these data.

FOLLOWING moderately large earthquakes seismic waves are observed worldwide; the recordings of these disturbances constitute the primary data source for studies of the Earth's internal structure. Under the hypothesis of isotropy, the physical parameters to which such observations are sensitive are the bulk modulus $\kappa(r, \theta, \varphi)$, the shear modulus $\mu(r, \theta, \varphi)$, and density $\rho(r, \theta, \varphi)$, where r, θ, φ are radius, colatitude and longitude. To accommodate dissipative effects κ and μ may be thought of as possessing small imaginary parts: $\kappa = \kappa_0(1 + iQ_\kappa^{-1})$, $\mu = \mu_0(1 + iQ_\mu^{-1})$ where κ_0, μ_0, Q_κ, Q_μ are real and have a weak dependence on frequency[1,2].

Studies since the beginning of the century have sought to determine the spherically symmetric parts of the parameter distributions $\bar{\rho}_0(r)$, $\bar{\kappa}_0(r)$, $\bar{\mu}_0(r)$, $\bar{Q}_\kappa(r)$, $\bar{Q}_\mu(r)$, resulting in spherical models of the Earth which are close to optimal in predicting a very wide range of seismic observations. Remaining discrepancies between observations and model predictions are largely due to deviations of the Earth from spherical symmetry, and while such deviations are relatively small, they constitute the principal observable evidence of processes taking place in the Earth's interior; as such, they have become a major focus of seismological research.

Here we take the velocities of shear (S) and longitudinal (P) waves: $v_s = [\mu/\rho]^{1/2}$, $v_P = [(\kappa + \frac{4}{3}\mu)/\rho]^{1/2}$ together with the density, ρ, to be the fundamental mechanical parameters, and write $v_s = \bar{v}_s[1 + \varepsilon_s(r, \theta, \varphi)]$, $v_P = \bar{v}_P[1 + \varepsilon_P(r, \theta, \varphi)]$ $\rho = \bar{\rho}[1 + \varepsilon_\rho(r, \theta, \varphi)]$ where $\bar{v}_S$, $\bar{v}_P$ and $\bar{\rho}$ are taken from a spherically symmetric reference Earth model; ε_S, ε_P and ε_ρ provide a dimensionless parameterization of heterogeneity.

The principal subdivisions of the Earth are the crust and upper mantle ($5{,}701 \leq r \leq 6371$ km), the lower mantle ($3{,}480 \leq r \leq 5{,}701$ km), the fluid outer core ($1{,}221 \leq r \leq 3{,}480$ km) and the solid inner core ($0 \leq r \leq 1{,}221$ km). The free surface and the boundaries between these regions are subject to small deflections from sphericity; we write for the radii of these surfaces: $R_{FS} = \bar{R}_{FS}[1 + \delta_{FS}(\theta, \varphi)]$, $R_{CMB} = \bar{R}_{CMB}[1 + \delta_{CMB}(\theta, \varphi)]$, $R_{ICB} = \bar{R}_{ICB}[1 + \delta_{ICB}(\theta, \varphi)]$, where FS, CMB and ICB refer to the free surface, the core-mantle boundary and the inner core boundary.

In recent years there have been a number of studies of large scale heterogeneity in the Earth, based upon several different kinds of seismic data[3-16]. In particular we refer to models of lower mantle P-velocity based upon travel time residuals[4,6] and models of upper mantle S-velocity based on very long period waveforms[10,16]. We report conclusions based upon observations of spectral splitting of free oscillations, a phenomenon analogous to, for instance, the Zeeman effect in atomic physics, which results from rotation ellipticity and other asphericity of the Earth[17-24].

Masters and Gilbert[25] have made the surprising observation that the splitting width of the model ${}_{10}S_2$ is more than twice that accounted for by the effects of Coriolis forces and ellipticity. More recently, Ritzwoller and Masters[26] and Ritzwoller *et al.*[27] have shown that many other multiplets have anomalously large splitting widths, and have concluded that an axisymmetric structural anomaly in the outer core is required to explain the observations, while recognizing that such an anomaly is essentially ruled out by hydrodynamic and thermal considerations (J. Bloxham, personal communication)[28]. It is the existence of this large effect, signalling an exotic phenomenon in the core, which has provided the motivation for this study.

Here we present the first results of a technique which enables structural information to be derived from seismic spectra; in principle we solve the least-squares inverse problem for structural parameters using the observed spectra as data. Our current data set consists of some 770 spectra for 27 modes—both anomalously and normally split. This data set alone is insufficient to resolve all structural parameters or to construct unique models of the mantle, outer core and inner core. By making use of the information from previous studies, however, we are able to test certain hypotheses and to explore the class of models which are in basic agreement both with previous models of the mantle and with the modal data set. Initially we restrict consideration to isotropic earth models; our conclusion, however, is that the resulting models are sufficiently at variance with other geophysical evidence that the hypothesis of isotropy should be rejected.

We describe two distinct experiments. In the first experiment our aim is to assess the consistency of the modal data with existing mantle models. Taking the subset of 19 modes which are principally sensitive to mantle structure (although many have significant sensitivity to the outer core), we consider models in which v_P, v_S vary proportionally: $\varepsilon_S = \alpha_{SP}\varepsilon_P$, $\varepsilon_\rho = \alpha_{\rho P}\varepsilon_P$, where α_{SP} and $\alpha_{\rho P}$ are constants. Results from laboratory experiments on the change in rock properties with temperature[29] have sometimes been used[8,27] as trial values of α_{SP} and $\alpha_{\rho P}$: $\alpha_{SP} = 1.25$ and $\alpha_{\rho P} = 0.5$. The sensitivity of the modal data to mantle heterogeneity in v_S is much greater than its sensitivity to v_P and ρ. Consequently there is only limited resolution for the parameters α_{SP}, $\alpha_{\rho P}$; if, however, we accept the levels of v_P heterogeneity obtained in travel-time analyses[3,4,6] larger values of α_{SP} are needed: $2 \leq \alpha_{sP} \leq 3$.

Adopting the values $\alpha_{SP} = 2.0$ and $\alpha_{\rho P} = 0.5$, we invert the mantle mode data set for P-wave velocity in the mantle (for reasons to be discussed below the inversion is limited to the spherical harmonic expansion coefficients of degrees 0, 2 and 4) and compare the resulting distribution of heterogeneity in P-velocity with the previous models. Since the models show substantial similarity we conclude (1) that the mantle mode data are in basic agreement with the models based upon travel time residuals if $\alpha_{SP} \simeq 2.0$, and are in fact sufficient to reproduce these models to a fair degree; (2) that despite significant

sensitivity of the 'mantle' modes to outer core structure, heterogeneity in the outer core is not required.

The mantle model we obtain possesses only small zonal terms and is not able to account for anomalous splitting, whose cause, therefore must be sought in the core. In the second experiment our aim is to quantify the core anomalies which are required. Adopting a mantle model constrained to be close to M84A (ref. 10) in the upper mantle and to L02.56 (ref. 4) in the lower mantle ($\alpha_{SP}=2.0$, $\alpha_{\rho P}=0.5$) and to be consistent with mantle modes we then seek models of the core (including CMB and ICB) and further small adjustments in the mantle to adequately match the entire modal data set. Including, first, heterogeneity in both outer and inner core we find that some modes can be accommodated by large (~0.5%) heterogeneity in the outer core, but that when the data set is taken as a whole the inclusion of outer core heterogeneity leads to models inconsistent with some modes, particularly ${}_3S_2$, ${}_3S_1$ and ${}_2S_3$. Only when inner core heterogeneity is allowed to approach 5% and boundary perturbations of CMB and ICB are allowed to approach 8 km and 25 km can a consistent model be found. Moreover, with these levels of heterogeneity in the inner core and CMB it proves to be possible to dispense entirely with heterogeneity in the outer core. The conclusion of this experiment is first that a large axisymmetric structure, located in the core, is required; and second, that under the hypothesis of isotropy, the modal data require heterogeneity in the CMB, ICB and inner core of the size stated above.

However, these results conflict with recent measurements of the Earth's nutation periods[30] and with evidence from PcP and PKP travel times[31] and we are led to conclude that there is no acceptable isotropic model capable of explaining the modal observations.

The splitting function

In a spherical Earth model a spheroidal multiplet ${}_nS_l$ is characterized by its angular order l (analogous to orbital angular momentum in atomic physics) and radial order n. Its eigenfrequency ${}_n\omega_l$ is $(2l+1)$-fold degenerate, and its singlets are labelled by their azimuthal order $m(-l\leq m\leq l$; analogous to magnetic quantum number).

Rotation, ellipticity, or other structural asphericity removes this degeneracy, leading to singlet eigenfrequencies ${}_n\omega_l+{}_n\delta\omega_l^i$ $(i=1,2,\ldots 2l+1)$. The frequency perturbations ${}_n\delta\omega_l^i$ may be calculated as the eigenvalues of the splitting matrix:

$$\mathbf{H}_{mm'}=\Omega\beta\delta_{mm'}+\bar{\omega}\sum_{st}^{2l}c_{st}(2l+1)\frac{(2s+1)^{1/2}}{2\pi^{1/2}}\times(-1)^m\begin{pmatrix}l & l & s\\ -m & m' & t\end{pmatrix}\begin{pmatrix}l & l & s\\ 0 & 0 & 0\end{pmatrix} \quad (1)$$

where the Wigner 3-j symbol[32] has been employed; Ω is the Earth's rotational angular velocity and β is the Coriolis splitting parameter[19]. The quantities c_{st} are linearly related to the Earth's heterogeneity of spherical harmonic order s and degree $t(-s\leq t\leq s)$:

$$c_{st}=\delta_{s2}\delta_{t0}c^e+\int_0^a\{E_P^s(r)\varepsilon_P^{st}(r)+E_S^s(r)\varepsilon_S^{st}(r)+E_\rho^s(r)\varepsilon_\rho^{st}(r)\}dr+\sum_h D_h^s\delta_h^{st} \quad (2)$$

where the first term represents the theoretical contribution of ellipticity, and $\varepsilon_P^{st}(r)$, $\varepsilon_S^{st}(r)$, $\varepsilon_\rho^{st}(r)$, δ_h^{st} $(h=\mathrm{FS,CMB,ICB})$ are the spherical harmonic expansion coefficients of ε_P, ε_S, ε_ρ and δ_h, excluding the contribution of ellipticity. In (2) a is the radius of the Earth and the kernels $E_P^s(r)$, $E_S^s(r)$, $E_\rho^s(r)$ and D_h^s are given by known expressions, in terms of the eigenfunction of a given multiplet[3].

A component of elastic displacement coresponding to a particular isolated multiplet can be written as a function of time[33]:

$$u(t)=\mathrm{Re}[\exp(i\bar{\omega}t)\cdot\mathbf{r}\cdot\exp(i\mathbf{H}t)\cdot\mathbf{s}] \quad (3)$$

where $\mathbf{r}$ and $\mathbf{s}$ are $(2l+1)$-dimensional vectors, characterizing the receiver and the source, and $\mathbf{H}$ is the $(2l+1)\times(2l+1)$ splitting matrix of equation (1).

Equations (1) and (3) give the (nonlinear) relation between an observed seismogram and the coefficients c_{st}, and equation (2) gives the (linear) relation between these coefficients and the model parameters. Because of selection rules satisfied by the 3-j symbols in (1), the summation over s contains only terms of even s; $s=0, 2, 4, \ldots 2l$ (refs 34, 35).

The quantities c_{st} $(s=0, 2, \ldots .2l; -s\leq t\leq s)$ may be thought of as the spherical harmonic expansion coefficients of a certain function, which is related to the local heterogeneity through the radially dependent kernels in (2). For a given multiplet we define:

$$\gamma(\theta,\varphi)=\sum_{s=0}^{2l}\sum_{t=-s}^{s}c_{st}\,Y_s^t(\theta,\varphi)$$

which we term the *splitting function*[36] of the multiplet, since knowledge of the splitting function is equivalent to knowledge of the splitting matrix $\mathbf{H}$.

Using (1) and (3) it is straightforward to formulate the discrete, nonlinear, least squares inverse problem for the splitting function, using as data all available spectra for the multiplet; the problem is linearized and solved iteratively. The resulting coefficients c_{st} constitute essentially model independent constraints on the three dimensional structure of the Earth of degree s and order t (the inferred values c_{st} will depend upon the source parameters and reference model used, but weakly). Using this technique we have retrieved the splitting functions of some 27 multiplets, with varying degrees of resolution (A similar technique has been employed by Ritzwoller *et al.*[27] in the estimation of the c_{20} coefficients alone). Difficulties in completely resolving the splitting functions using the current data set have led us to pursue, in parallel, a second technique in which inversion for structural perturbations is carried out directly. Earth models are first constructed by linear inversion, using the derived splitting functions as data, and these models are then adjusted iteratively to achieve agreement with the spectra for all multiplets.

Data and inversion results

For a study of this kind we require very long period seismograms produced by large earthquakes and recorded digitally. The limiting factors are that such data have been collected only since 1976 and for rather few stations, and that large earthquakes are rare. The principal source is the International Deployment of Accelerometers (IDA) network[37], which provided all the data included in this study. All available traces for the ten largest events since 1977 were employed.

In Fig. 1 are shown some examples of data and theoretical predictions in three spectral windows, each containing one or two multiplets. In Fig. 1*a–c* the theoretical spectra include only the effects of rotation and ellipticity while in Figs. 1*d–f* the theoretical predictions are based on splitting functions obtained by inversion. It will be noted that, owing to attenuation and finite record length, it is not possible to resolve the singlets within a multiplet in individual spectra. The power of the splitting function inversion technique is that it allows all spectra for a given multiplet to be simultaneously brought to bear in unmasking the underlying fine structure of the spectrum. Both amplitude and phase are very poorly predicted by rotation and ellipticity alone (Fig. 1*a–c*), often giving a variance ratio (squared misfit/squared data) greater than 1. For the three spectral windows shown the inversion results are based on 19, 57 and 30 traces respectively, and for all data the (initial, final) variance ratios are (1.79, 0.30), (0.69, 0.19) and (0.90, 0.25). Table 1 gives these parameters for all the spectral windows used.

The splitting width of ${}_{13}S_2$ is estimated to be anomalous by a factor of R = 2.4 (Fig. 1*a*, *d*), in agreement with the value

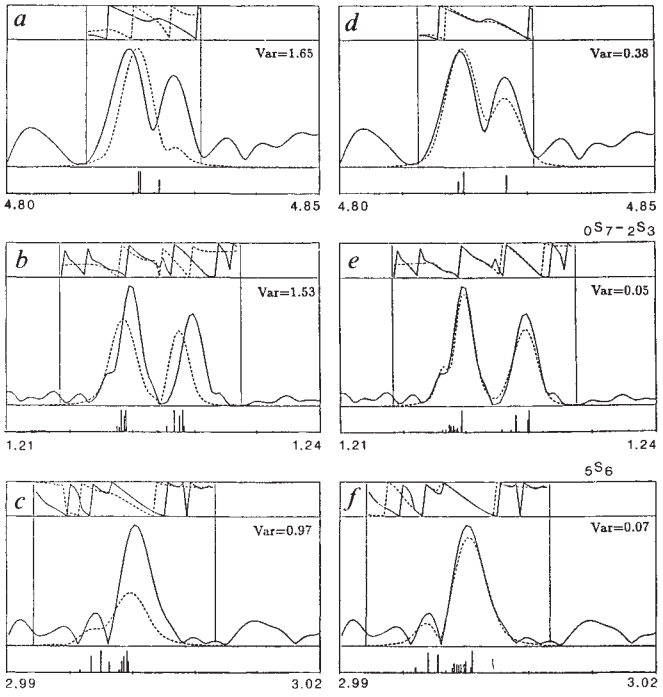

Fig. 1 Examples of data (solid lines) and synthetic spectra (dashed lines) in three spectral windows, each containing one or two multiplets. The range of the (horizontal) frequency axis is indicated in mHz. The spectra are represented in terms of phase in the interval $(-\pi, \pi)$ (top panel of each figure), and amplitude on an arbitrary scale (middle panel). Vertical bars in the bottom panels indicate the frequencies and relative amplitudes of the singlets contributing to the theoeretical spectra. The variance ratio (Var) is a measure of the misfit between the observed and synthetic traces shown. In *a–c* the theoretical traces incorporate only the effects of rotation and ellipticity, while in *d–f* the splitting functions found by inversion are employed. A Hann window has been employed to enhance resolution in frequency[38].

reported by Ritzwoller *et al.* ($R = 2.3$)[27]. Since a primary motivation of this study is to find an explanation of such highly anomalous modes as $_{13}S_2$, $_3S_2$, which are sensitive only to heterogeneity of degree 0, 2, 4 and since the data set has finite resolution, we limit our inversions both for splitting functions and for model parameters to these degress, despite the fact that modes of angular order greater than 2 are sensitive to higher degrees; for similar reasons we allow only for degree 0 in the imaginary parts of the splitting functions—corresponding to a spherically symmetric correction in attenuation.

The source parameters used in calculating synthetic spectra are those determined by the centroid-moment tensor technique[39,40], subject to corrections in scalar moment using the modal data set; these multiplicative corrections are close to unity and play only a minor role in reducing the data variance; similarly attentuation corrections give small contributions. The large discrepancies in the amplitude spectra (Fig. 1) are accommodated, instead, by adjustment of the interference between closely spaced singlets.

The modes used in this study were selected to span a wide range in phase velocities and to be easily observable in many individual spectra. Notable modes which have been omitted here are the closely spaced pair $_{10}S_2$, $_{11}S_2$. These modes have eigenfunctions which are poorly predicted by current spherical models[25]. The observed mode can be obtained by taking a linear combination of eigenfunctions predicted by PREM[4], resulting in a mode very similar in its properties and its splitting to $_{13}S_2$ and having a Q of approximately 800. A more complete analysis of this mode will be presented elsewhere.

Table 1 Normal modes and variance ratios from different models

Mode	T	V_0	V_{Cst}	V_m	Rec
$_0S_3^\dagger$	2135	0.206	0.169	0.202	22
$^1S_3^\dagger$–$_3S_1^\dagger$	1061	0.436	0.302	0.456	37
$_0S_6^\dagger$	964	0.624	0.144	0.170	37
$_3S_2$	904	1.467	0.323	0.401	25
$_1S_4^\dagger$	851	0.400	0.325	0.329	35
$_0S_7^\dagger$–$_2S_3$	809	0.689	0.188	0.169	57
$_1S_5^\dagger$–$_2S_4^\dagger$	727	0.659	0.341	0.543	47
$_2S_5^\dagger$–$_1S_6^\dagger$	658	0.876	0.727	0.819	35
$_1S_7^\dagger$	604	0.880	0.282	0.359	38
$_1S_8^\dagger$	556	0.936	0.311	0.441	36
$_4S_3^\dagger$–$_2S_8^\dagger$	488	0.862	0.450	0.530	67
$_5S_3^\dagger$	461	0.554	0.377	0.472	11
$_5S_4^\dagger$	420	0.687	0.402	0.521	47
$_5S_5^\dagger$	370	0.708	0.349	0.439	58
$_3S_8^\dagger$–$_6S_3$	354	0.944	0.355	0.494	39
$_5S_6^\dagger$	332	0.900	0.252	0.476	30
$_9S_3$	281	1.020	0.302	0.433	15
$_{11}S_4$	210	1.406	0.406	0.539	22
$_{13}S_2$	207	1.790	0.304	0.377	19
$_{11}S_5$	197	1.140	0.556	0.747	24
$_{13}S_3$	193	1.069	0.398	0.421	21

The frequency windows are ordered by decreasing period in seconds (T). The 'mantle modes' are indicated by †. V_0 is the variance ratio (squared misfit/squared data) obtained using the reference model PREM[42] and incorporating only the effects of rotation and ellipticity (Fig. 1*a–c*); V_{Cst} is the variance obtained using the splitting functions retrieved by nonlinear inversion (cf. Fig. 1*d–f*); V_m is from the anisotropic model discussed in the text. The number of records used for each spectral window is indicated.

Aspherical models

Before describing the results of inversion for model parameters, we first discuss some examples of splitting functions retrieved by the technique outlined before, together with their associated kernels, which quantify the sensitivity of the splitting function to perturbations in ε_P, ε_S and ε_ρ as a function of radius and to δ_{FS}, δ_{CMB} and δ_{ICB}.

The modes $_1S_7$, $_0S_6$ and $_1S_8$ (see Fig. 2*a–c*) are characterized by high sensitivity to S-velocity in the lower mantle. Note that if $\alpha_{SP} = 2.0$, a truer representation of the importance of E_S, relative to E_P, would be obtained by multiplying E_S by this factor. The splitting functions of these modes are similar and are dominated by a degree 2 pattern known to be characteristic of the lower mantle[4]. Notwithstanding significant sensitivity in the outermost core these splitting functions do not possess the large axisymmetric terms characteristic of anomalously split modes, suggesting that this region is not responsible for anomalous splitting.

The multiplets $_{13}S_3$, $_6S_3$ and $_{13}S_2$, on the other hand (Fig. 2*d–f*), possess large c_{20} terms (the harmonic $P_2^0(\cos\theta)$). Modes $_{13}S_3$ and $_{13}S_2$ have rather similar kernels, but $_{13}S_2$ shows a larger effect. The fact that the kernels for $_{13}S_2$ are larger in the inner core is suggestive of an inner core origin for the c_{20} anomaly.

The multiplets $_3S_1$, $_3S_2$ and $_2S_3$ (Fig. 2g–i) possess sensitivity throughout the Earth and their kernels are, in some respects, similar. These modes have very different splitting functions, however, which constitute rather delicate discriminants between hypotheses concerning the location of the heterogeneity. Mode $_3S_1$ (Fig. 2*g*), which is insensitive to degree 4, has a very small splitting function. Its insensitivity to lower mantle structure is probably due to cancellation of P and S effects, since the kernels are of opposite sign and roughly $E_P \sim -2\,E_S$; the fact that its kernels are large in the outer core makes it difficult to place significant heterogeneity of degree 2 in this region. Mode $_3S_2$

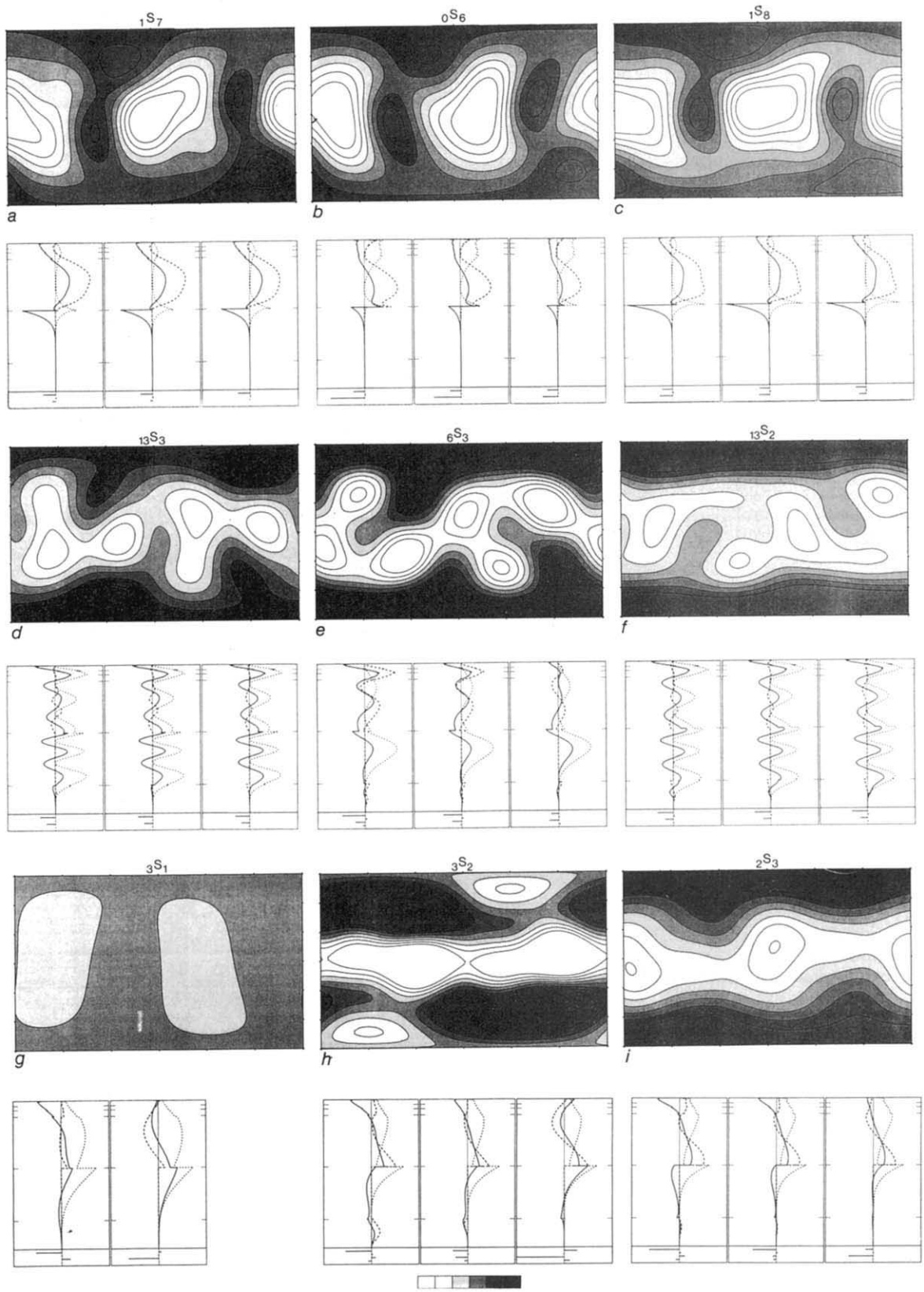

Fig. 2 Examples of splitting functions and differential kernels for 9 of the multiplets used. The kernels E^s_P (solid), E^s_P (dotted) and E^s_S (dashed) indicate, on a uniform scale and as a function of radius, running vertically, the sensitivity of the splitting function to a 1% change in ρ, v_P or v_s. The four horizontal bars in the bottom panel of each figure represent, on the same scale, the sensitivity to a deflection of the boundaries by 100 km. These boundaries, from top to bottom, are the free surface, the 670 km discontinuity, the core-mantle boundary and the inner core boundary. The kernels shown (from left to right) correspond to heterogeneity of harmonic degree 0, 2, 4. The line corresponding to a degree 4 perturbation of CMB in h(mode $_3S_2$) exceeds the scale by 18%. The splitting functions are represented in a global linear map projection (ordinate latitude, abcissa longitude) centred on longitude 180°. The contouring interval is 0.067%; the maximum of the scale of shading, which is saturated in some cases, is 0.2%; darker shading corresponds to positive values.

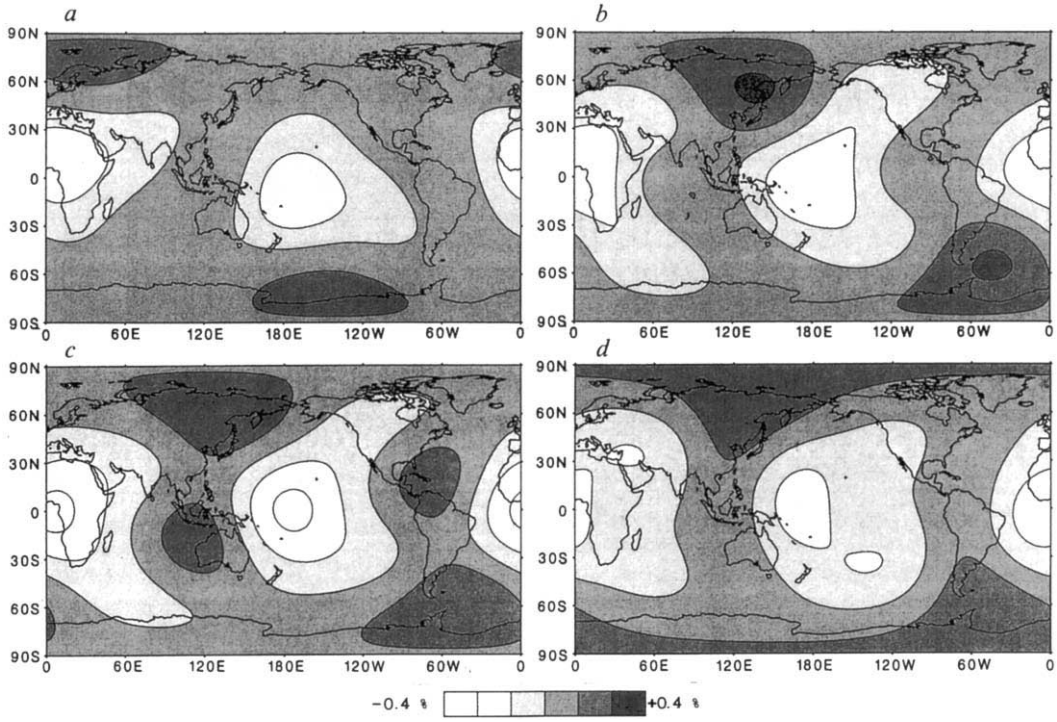

Fig. 3 Comparison of Model 1 (left; *a*, *c*) with the travel-time model V3.I of Morelli & Dziewonski[6] (right; *b*, *d*) at depths 2,700 km (top; *a*, *b*) and 2,300 km (bottom; *c*, *d*). Correlation coefficients are $cc_{ab} = 0.74$, $cc_{cd} = 0.88$. The models correspond to completely independent inversions of very different data sets. The Model V3.I contains all degrees up to $s = 6$, but only degrees 2 and 4 are shown.

has, among the multiplets studied, by far the greatest components of degree 4 (Fig. 2*h*). Its great sensitivity to a degree 4 deflection of the core-mantle boundary suggests that the CMB can give a large contribution for this mode. Its kernels in the mantle and in the outermost core are similar to those of ${}_2S_3$ (Fig. 2*i*), which, in contrast, has a splitting function dominated by c_{20} and, to a lesser extent by other terms of degree 2. The correlation coefficients of the degree 2 terms, omitting c_{20}, of the splitting function of ${}_2S_3$ with those of the 'mantle' modes ${}_1S_7$, ${}_0S_6$ and ${}_1S_8$ (Fig. 2*a*–*c*) are 0.96, 0.83 and 0.97, respectively – a strong indication of a common origin for these terms in the mantle. It should be noted that the inversion for each spectral window is carried out independently of other spectral windows, and thus similarities between the derived splitting functions of different multiplets which sample the Earth in a similar way provides confirmation of the accuracy of the results.

The mantle. Taking as data the splitting functions of 19 mantle modes we first invert for a mantle model (see above) using $\alpha_{SP} = 2.0$, $\alpha_{\rho P} = 0.5$. The problem is made discrete by parameterising ε_P^{st} (and hence ε_S^{st}, ε_ρ^{st}) as combinations of orthogonal polynomials of degrees up to 6 defined on the interval $[R_{CMB}, R_{FS}]$. The data set proves insufficient to completely resolve all 105 parameters and we employ a stochastic inverse, which is equivalent to incorporating artificial *a priori* information that the parameters are small. The trade-off between model size and variance reduction leads us to choose a level of damping corresponding to a model possessing 43 degrees of freedom. This model will be referred to hereafter as Model 1. The v_P anomalies in Model 1 have a similar size (in the sense of the r.m.s.) to the travel time model L02.56 of Dziewonski[4] and the similar model V3.1 of Morelli and Dziewonski[6].

Here we compare Model 1 with the model V3.I[6]. At the depth 2,700 km ($r = 3{,}671$ km, Fig. 3*a*, *b*) the dominant features of the models are in fairly good agreement (correlation coefficient on 13 degrees of freedom $cc = 0.74$), while at 2,300 km ($r = 4{,}071$ km, Fig. 3*c*–*d*) the agreement is somewhat better ($cc = 0.88$). The fact that the travel time model at 2,700 km agrees remarkably in shape with the splitting functions of mantle modes (Figs 3*b*, 2*b*; $cc = 0.82$) and that the Model 1 varies relatively slowly with depth in the lowermost mantle (Fig. 3*a*–*b*) suggests that lack of resolution, rather than any major inconsistency of the travel time model with the splitting function results, is responsible for the poorer agreement at 2,700 km.

In Fig. 4 Model 1 is compared with two other models at depth 1,300 km ($r = 5071$ km). Fig. 4*c* is taken from a recent model of Woodhouse and Dziewonski[16] based upon mantle waves and long period multiple SH reflected body waves, for the upper 1,500 km of the mantle. Since the model is for S-velocity, it is divided by $\alpha_{SP} = 2.0$ in order to make the comparison with P. In this case the correlation coefficients of Model 1 with the two other models are somewhat lower, but still highly significant ($cc = 0.56$, $cc = 0.63$).

The core. As described previously, we construct a model which is designed to be close to L02.56[4] and M84A[10] in the mantle and to match the modal data. It is also required to predict the observed geoid and to be in mechanical equilibrium with vanishing deviatoric stress in the outer core. The core mantle boundary has large components in the harmonics $P_2^0(\cos\theta)$, $P_4^0(\cos\theta)$, which are required to explain the splitting function of ${}_3S_2$. The inner core boundary perturbations are dominated by degree 2 and exceed 25 km; heterogeneity within the inner core is dominated by degree 2 and exceeds 6% near the top of the inner core, where ε_P reaches its amximum. The axisymmetric anomaly responsible for anomalous splitting is contained in the CMB, ICB and within the inner core. While a model of this kind is capable of explaining most of the modal observations the existence of large CMB topography of degrees 2 and 4 is inconsistent with recent inferrences from geodetic data[30] and from travel times[31].

In Fig. 5 the sensitivities of the splitting function coefficients

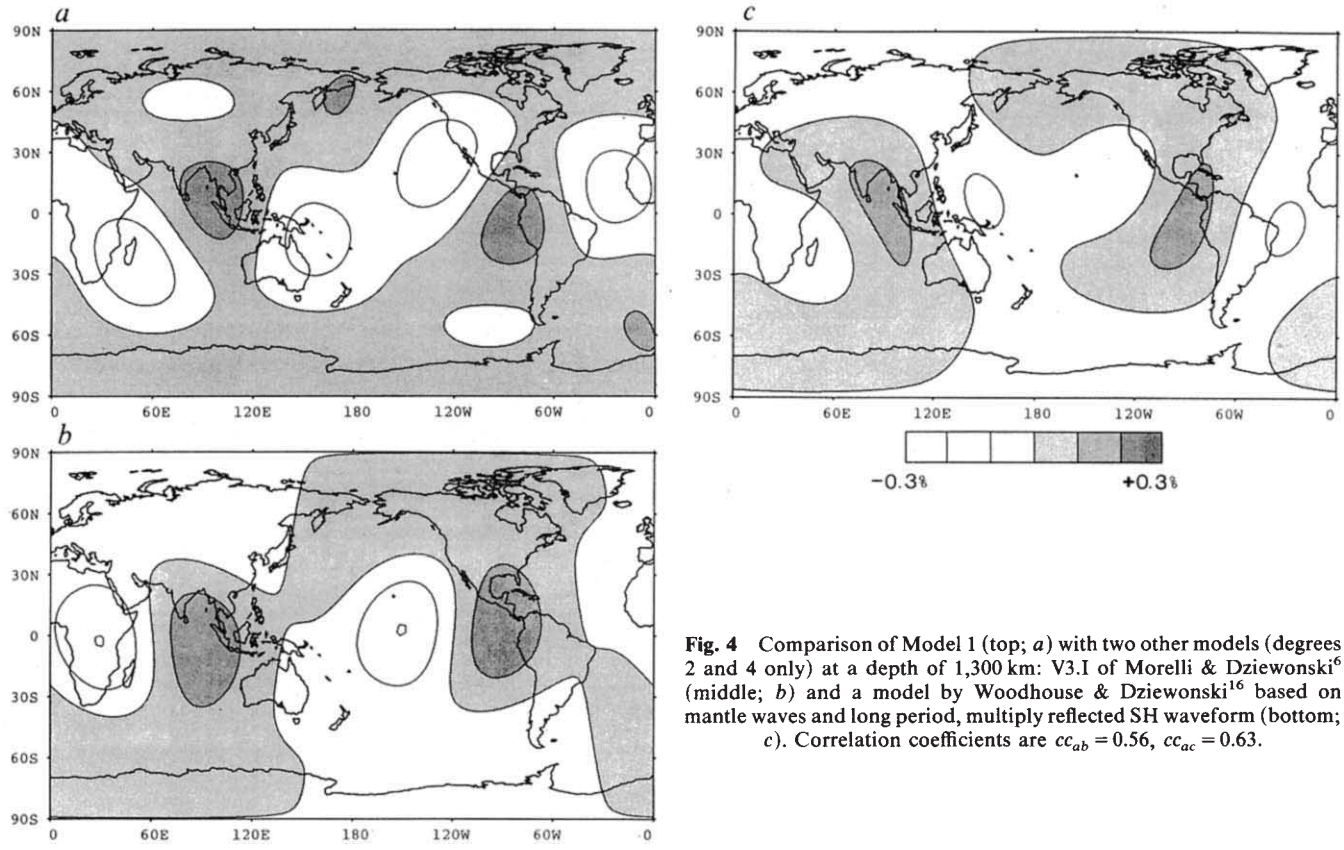

Fig. 4 Comparison of Model 1 (top; *a*) with two other models (degrees 2 and 4 only) at a depth of 1,300 km: V3.I of Morelli & Dziewonski[6] (middle; *b*) and a model by Woodhouse & Dziewonski[16] based on mantle waves and long period, multiply reflected SH waveform (bottom; *c*). Correlation coefficients are $cc_{ab} = 0.56$, $cc_{ac} = 0.63$.

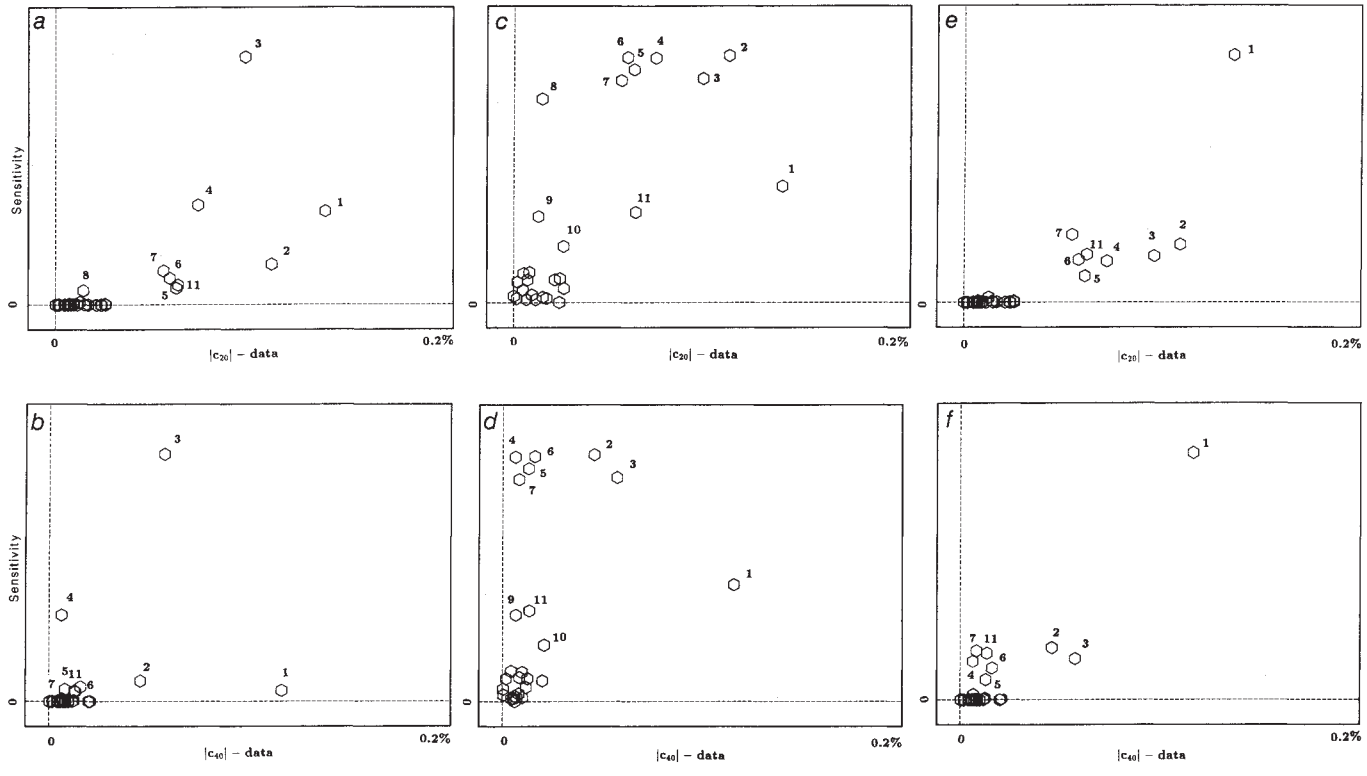

Fig. 5 Plots of the sensitivities of the splitting function coefficients c_{20} (top) and c_{40} (bottom) to structural perturbations in the inner core (left) outer core (middle) and to inner core zonal anisotropy (right). Normal mode multiplets are indicated by numerals: 1: ${}_3S_2$; 2: ${}_6S_3$; 3: ${}_{13}S_2$; 4: ${}_{13}S_3$; 5: ${}_{11}S_5$; 6: ${}_{11}S_4$; 7: ${}_9S_3$; 8: ${}_3S_1$; 9: ${}_5S_3$; 10: ${}_2S_4$; 11: ${}_2S_3$.

c_{20}, c_{40} to structural perturbations in the inner core (Fig. 5*a*, *b*); outer core (*c*, *d*) and to inner core anistoropy (*e*, *f*) are plotted against the observed magnitudes of these coefficients. While it is not possible to draw rigorous conclusions from these, they do provide useful indicators of what kinds of structure are likely to provide plausible explanations of anomalous splitting, and serve as a focal point for discussion.

In Fig. 5*a*, *b*, the ordinate is the root mean square sensitivity to inner core ε_S and ε_P perturbations of degree 2 and 4 respectively; a radial dependence proportional to r^2 is assumed. Modes which do not penetrate the inner core have almost vanishing sensitivities and small observed coefficients. Modes which lie near one of the axes but far from the other represent potential problems for an inner core explanation of anomalous splitting. The mode ${}_3S_2$, for instance, has very small sensitivity to inner core structure but a very large coefficient c_{40} (Fig. 5*b*). In the model discussed above, ths mode could be explained only by CMB topography. The modes ${}_6S_3$ and ${}_{13}S_2$ have coefficients of similar size for both degrees, but very different sensitivities. For this reason they can both be accommodated in the model only by complex radial dependence and by cancellation among ε_P, ε_S and ε_ρ effects for ${}_{13}S_2$.

Figure 5*c*, *d* shows similar plots corresponding to an outer core ε_P anomaly independent of radius. As noted above, ${}_3S_1$ has a large sensitivity to such a structure and a very small splitting function. The model proposed by Ritzwoller *et al.*[27] accommodates this mode by placing a degree 2 anomaly in the mantle which cancels the core effect; it is our conclusion, however, that such an anomaly is inconsistent with the constraints placed on mantle structure by travel time studies[4–6] and by mantle modes. For degree 4 (Fig. 5*d*), modes ${}_{13}S_3$, ${}_{11}S_5$, ${}_{11}S_4$ and ${}_9S_3$ indicate very small heterogeneity but ${}_3S_2$ requires a large effect. An outer core anomaly would need to possess a complicated radial dependence to reconcile the data for degree 4.

Finally, Fig. 5*e*, *f* shows sensitivities to axially symmetric aniostropy in the inner core. There is a large number of anisotropic parameters and again the rms sensitivity is used (the details of this calculation will be presented elsewhere). It will be noted that Fig. 5*e*, *f* shows a much more coherent pattern. In particular, the highly anomalous mode ${}_3S_2$ has the greatest sensitivity to inner core anisotropy and modes having small degree 4 coefficients also have small sensitivities. These figures show that inner core anisotropy would provide a rather natural explanation of the character of the anomalous split modes. Table 1 gives the data variances of a model constrained to be close to M84A (ref. 10) and L02.56 (ref. 4) in the mantle ($\alpha_{SP} = 2.0$, $\alpha_{\rho P} = 0.5$) and to have CMB topography close to that determined by Morelli and Dziewonski[31] and possessing an anisotropic inner core. It will be seen that the single hypothesis of axially symmetric inner core anistropy yields a rather satisfactory fit to the data. A more complete discussion of anisotropic models will be presented elswhere.

Conclusions

The splitting functions of free oscillations provide linear constraints on three dimensional Earth models which are (essentially) model independent. Given sufficient data they can be vary accurately determined. While the quantity of data now available is marginal for the resolution of some multiplets, the new networks currently under development[42–45], operating over, say, a 10 year span should enable a large number of splitting functions to be as well determined as the geoid, adding greatly to our knowledge of the Earth's internal structure.

The current data set has proved capable of resolving some features of mantle structure already documented using travel-time techniques. In order to satisfy the data for core modes significant zonal heterogeneity in the core is required. Under the hypothesis of isotropy, variations of several percent in inner core properties and undulations of 8 and 23 km on the core-mantle boundary and inner core boundary are required. The alternative hypothesis that the inner core is anisotropic, having an axis of symmetry coincident with the Earth's rotation axis, offers a more natural explanation of the modal observations which, in addition, does not conflict with other data or with the expected homogeneity of the outer core.

We thank J. Berger, D. C. Agnew and the staff of the IDA Project for providing us with the data used in this study. We thank with our colleagues, J. Bloxham, A. M. Dziewonski, A. Morelli and R. J. O'Connell for numerous discussions and we thank A. Morelli and A. M. Dziewonski for allowing us to make use of their unpublished model V3.I. We thank M. Ritzwoller, G. Masters and F. Gilbert for a preprint of their recent paper[27] and F. A. Dahlen and F. Gilbert, G. Masters and M. Ritzwoller for their reviews. This reasearch was carried out with the support of the NSF under the grant EAR85-11400.

Received 1 August; accepted 20 November 1986.

1. Futterman, W. I. *J. geophys. Res.* **67**, 5279–4291 (1962).
2. Liu, H-P., Anderson, D. L. & Kanamori, H. *Geophys. J. R. astr. Soc.* **47**, 41–58 (1976).
3. Dziewonski, A. M., Hager, B. H. & O'Connell, R. J. *J. geophys. Res.* **82**, 239–255 (1977).
4. Dziewonski, A. M. *J. geophys. Res.* **89**, 5929–5952 (1984).
5. Clayton, R. W. & Comer,R. P. *Eos* **64**, 776 (1983).
6. Morelli, A. & Dziewonski, A. M. *Eos* **67**, 311 (1986).
7. Creager, K. C. & Jordan, T. H. *Eos* **67**, 311 (1986).
8. Masters, G., Jordan, T. H., Silver, P. G. & Gilbert, F. *Nature* **298**, 609–613 (1982).
9. Woodhouse, J. H. *Proc. Enrico Fermi Int. Sch. Phys.* **85**, 366–397 (1983).
10. Woodhouse, J. H. & Dziewonski, A. M. *J. geophys. Res.* **89**, 5953–5986 (1984).
11. Nakanishi, I. & Anderson, D. L. *Bull. seism. Soc. Am.* **72**, 1185–1194 (1982).
12. Nakanishi, I. & Anderson, D. L. *J. geophys. Res.* **88**, 10267–10283 (1983).
13. Nakanishi, I. & Anderson, D. L. *Geophys. J. R. astr. Soc.* **78**, 573–618 (1984).
14. Nataf, H.-C., Nakanishi, I. & Anderson, D. L. *Geophys. Res. Lett.* **11**, 109 (1984).
15. Tanimoto, T. & Anderson, D. L. *J. geophys. Res.* **90**, 1842 (1985).
16. Woodhouse, J. H. & Dziewonski, A. M. *Eos* **67**, 307 (1986).
17. Ness, N. F., Harrison, C. S. & Slichter, L. J. *J. geophys. Res.* **66**, 621–629 (1961).
18. Benioff, H., Press, F. & Smith, S. W. *J. geophys. Res.* **66**, 605–619 (1961).
19. Backus, G. E. & Gilbert, F. *Proc. natn. Acad. Sci. U.S.A.* **47**, 362–371 (1961).
20. Pekeris, C. L., Alterman, A. & Jarosch, M. *Phys. Rev.* **122**, 1692–100 (1961).
21. Dahlen, F. A. *Geophys. J. R. astr. Soc.* **16**, 329–367 (1968).
22. Dahlen, F. A. *J. geophys. Res.* **81**, 4951–4956 (1976).
23. Woodhouse, J. H. & Dahlen, F. A. *Geophys. J. R. astr. Soc.* **53**, 335–354 (1978).
24. Dahlen, F. A. & Sailor, R. V. *Geolphys, J. R. astr. Soc.* **58**, 609–623 (1979).
25. Masters, G. & Gilbert, F. *Geophys. Res. Lett.* **8**, 569–571 (1981).
26. Ritzwoller, M. & Masters, G. *Eos* **65**, 1003 (1984).
27. Ritzwoller, M., Masters, G. & Gilbert, F. *J. geophys. Res.* **91**, 10203–10228 (1986).
28. Stevenson, D. *Geophys. J. R. astr. Soc.* (submitted).
29. Anderson, O. L., Schreiber, E., Lieberman, R. C. & Soga, M. *Rev. Geophys. Space Phys.* **6**, 491–524 (1968).
30. Gwinn, C. R., Herring, T. A. & Shapiro, I. I. *J. geophys. Res.* **91**, 4755–4765 (1986).
31. Morelli, A. & Dziewonski, A. M. *Nature* (in the press).
32. Edmonds, A. R. *Angular Momentum in Quantum Mechanics* (Princeton University Press, Princeton, 1960).
33. Woodhouse, J. H. & Girnius, T. P. *Geophys. J. R. astr. Soc.* **68**, 653–673 (1982).
34. Zharkov, B. N. & Lyubimov, V. M. *Izv. Acad. Sci. USSR Phys. Solid Earth* **10**, 613–618 (1970).
35. Madariaga, R. thesis, MIT (1971).
36. Woodhouse, J. H. & Giardini, D. *Eos Trans. AGU* **66**, 300 (1985).
37. Agnew, D. C. *et al. Eos* **67**, 203–212 (1986).
38. Dahlen, F. A. *Geophys. J. R. astr. Soc.* **69**, 537–549 (1982).
39. Dziewonski, A. M., Chou, T.-A. & Woodhouse, J. H. *J. geophys. Res.* **86**, 2825–2852 (1981).
40. Dziewonski, A. M. & Woodhouse, J. H. *J. geophys. Res.* **88**, 3247–3271 (1983).
41. Dziewonski, A. M. & Anderson, D. L. *Phys. Earth Planet. Inter.* **25**, 297–356 (1981).
42. Romanowicz, B., Cara, M., Fels, J. F. & Rouland, D. *Eos* **65**, 753 (1984).
43. Nolet, G., Romanowicz, B., Kind, R. & Wielandt, E. *ORFEUS science plan, report, Observ. and Res. Facil. for Eur. Seismol.* (*ORFEUS*), Luxembourg (1985).
44. Smith, S. W. *Eos* **67**, 213–219 (1986).
45. Romanowicz, B. & Dziewonski, A. M. *Eos* **67**, 541 (1986).